Constraining surface carbon fluxes using in situ measurements of carbonyl sulfide and carbon dioxide

Citation	Berkelhammer, M., D. Asaf, C. Still, S. Montzka, D. Noone, M. Gupta, R. Provencal, H. Chen, and D. Yakir (2014), Constraining surface carbon fluxes using in situ measurements of carbonyl sulfide and carbon dioxide. Global Biogeochemical Cycles, 28, 161–179. doi:10.1002/2013GB004644
DOI	10.1002/2013GB004644
Publisher	American Geophysical Union
Version	Version of Record
Citable Link	http://hdl.handle.net/1957/47981
Terms of Use	http://cdss.library.oregonstate.edu/sa-termsofuse

Constraining surface carbon fluxes using in situ measurements of carbonyl sulfide and carbon dioxide

M. Berkelhammer[1,2], D. Asaf[3], C. Still[4], S. Montzka[5], D. Noone[1], M. Gupta[6], R. Provencal[6], H. Chen[7,8], and D. Yakir[3]

[1]Department of Atmospheric and Oceanic Sciences, Cooperative Institute for Research in Environmental Sciences, University of Colorado Boulder, Boulder, Colorado, USA, [2]Now at Department of Earth and Environmental Sciences, University of Illinois, Chicago, Illinois, USA, [3]Department of Environmental Sciences and Energy Research, Weizmann Institute of Science, Rehovot, Israel, [4]Forest Ecosystems and Society, Oregon State University, Corvallis, Oregon, USA, [5]Earth System Research Laboratory, Global Monitoring Division, National Oceanic and Atmospheric Administration, Boulder, Colorado, USA, [6]Los Gatos Research Inc., Mountain View, California, USA, [7]Center for Isotope Research, University of Groningen, Groningen, Netherlands, [8]Cooperative Institute for Research in Environmental Sciences, University of Colorado, Boulder, Colorado, USA

Abstract Understanding the processes that control the terrestrial exchange of carbon is critical for assessing atmospheric CO_2 budgets. Carbonyl sulfide (COS) is taken up by vegetation during photosynthesis following a pathway that mirrors CO_2 but has a small or nonexistent emission component, providing a possible tracer for gross primary production. Field measurements of COS and CO_2 mixing ratios were made in forest, senescent grassland, and riparian ecosystems using a laser absorption spectrometer installed in a mobile trailer. Measurements of leaf fluxes with a branch-bag gas-exchange system were made across species from 10 genera of trees, and soil fluxes were measured with a flow-through chamber. These data show (1) the existence of a narrow normalized daytime uptake ratio of COS to CO_2 across vascular plant species of 1.7, providing critical information for the application of COS to estimate photosynthetic CO_2 fluxes and (2) a temperature-dependent normalized uptake ratio of COS to CO_2 from soils. Significant nighttime uptake of COS was observed in broad-leafed species and revealed active stomatal opening prior to sunrise. Continuous high-resolution joint measurements of COS and CO_2 concentrations in the boundary layer are used here alongside the flux measurements to partition the influence that leaf and soil fluxes and entrainment of air from above have on the surface carbon budget. The results provide a number of critical constraints on the processes that control surface COS exchange, which can be used to diagnose the robustness of global models that are beginning to use COS to constrain terrestrial carbon exchange.

1. Introduction

Better constraints on the processes that control the magnitude of the terrestrial carbon sink are needed in order to improve understanding of climate-carbon feedbacks [*Schimel et al.*, 2001] and guide climate change mitigation strategies aimed at using forests for carbon sequestration [*Barford et al.*, 2001]. Studies that have reconstructed temporal variations in the terrestrial carbon cycle using, for example, flux [*Urbanski et al.*, 2007] or flask [*Ballantyne et al.*, 2012] data have revealed long-term trends and interannual variability in carbon uptake that are not reproduced by the current carbon cycle models [*Friedlingstein et al.*, 2006]. This discrepancy highlights the presence of missing processes in the models which, in part, reflects the observational challenge of separating net ecosystem exchange into its constituent source and sink terms (i.e., terrestrial ecosystem respiration and gross primary production, respectively). Observations that can clearly delineate respiration and photosynthetic fluxes on subseasonal time scales are thus needed to develop empirical relationships between climate and carbon cycling, which can be utilized to diagnose model skill and improve their predictive capabilities [*Beer et al.*, 2010].

CO_2 and H_2O fluxes derived from the global network of eddy covariance sites are amongst the few observationally based data with high temporal resolution available on terrestrial carbon cycle fluxes [*Baldocchi et al.*, 2001]. However, because of the requirement for a highly turbulent atmosphere to accurately retrieve fluxes from this method, data gaps emerge during stable periods such as the night and early mornings [*Fisher et al.*, 2007; *Wilson et al.*, 2002; *Gu et al.*, 2005; *Berkelhammer et al.*, 2013]. The inability to accurately

retrieve nocturnal carbon fluxes leads to difficulties in constraining the respiration fluxes from soil. Attempts to overcome this issue have been pursued through the use of soil chambers, analysis of respiration during turbulent nights, utilization of the covariance of water and carbon fluxes, advection experiments, and measurements of isotope ratios in atmospheric CO_2 [*Lasslop et al.*, 2009; *Lavigne et al.*, 1997; *Scanlon and Kustas*, 2010; *Yakir and Wang*, 1996; *Loescher et al.*, 2006; *Aubinet et al.*, 2010]. Although there is qualitative agreement between many of these approaches, discrepancies are significant enough to warrant the investment associated with the development of independent methods to characterize the magnitude of CO_2 fluxes.

Measurements of the concentration or fluxes of carbonyl sulfide (COS) may provide a direct constraint on gross primary production (GPP) [*Blonquist et al.*, 2011; *Wohlfahrt et al.*, 2012; *Asaf et al.*, 2013]. The idea of this proxy originated from observational studies suggesting COS is directly consumed by vegetation [e.g., *Mihalopoulos et al.*, 1989]. An inventory of the covariation of COS and CO_2 over terrestrial sites from the National Oceanic and Atmospheric Administration (NOAA) flask network by *Montzka et al.* [2007] suggests the timing and amplitude of the COS seasonal cycle is consistent with plants being the dominant terrestrial sink and that the ratio of CO_2 to COS uptake is generally consistent between sites. A growing body of COS data support the idea that this could be used as a GPP proxy by showing (1) the uptake ratio between COS and CO_2 is common across species [*Stimler et al.*, 2010a; *Sandoval-Soto et al.*, 2005], (2) there is a lack of COS emissions by actively photosynthesizing plants (i.e., a retroflux) [*Wohlfahrt et al.*, 2012; *Simmons et al.*, 1999; *Stimler et al.*, 2010a], and (3) an emerging theoretical understanding of the physical (i.e., stomata) and enzymatic (i.e., carbonic anhydrase) pathway for COS consumption that agrees with the observed uptake ratio between COS and CO_2 [*Protoschill-Krebs et al.*, 1996; *Seibt et al.*, 2010]. These works based on both greenhouse and field observations find a covariance between COS fluxes and photosynthetic active radiation and humidity, implying a stomatal control for COS uptake. The stability of the ratio of COS to CO_2 uptake across species is understood to arise because the two species diffuse into leaves along a similar pathway to the mesophyll where carbonic anhydrase reacts with the molecules [*Protoschill-Krebs et al.*, 1996].

Recent field measurements by *Asaf et al.* [2013] show promising indications that COS can be used as a GPP proxy across a variety of ecosystems. The results from this seminal study find general agreement between GPP estimates derived from traditional CO_2 flux methods and COS data. However, at most of the ecosystems studied, COS-derived GPP was larger than the estimates derived from CO_2 fluxes. These differences may highlight a systematic bias in one or both of the approaches. For example, this discrepancy could arise if the soil CO_2 source is being overestimated or the soil COS sink is being underestimated. In order to properly assess where the differences arise between these methods and provide tighter constraints for global modeling of COS [*Berry et al.*, 2013; *Campbell et al.*, 2008], a number of existing issues regarding controls on the surface COS budget must still be addressed. These issues include (1) better constraints on COS fluxes from soils, senescent vegetation, and other nonvegetative sources [*Van Diest and Kesselmeier*, 2008; *Simmons et al.*, 1999; *Liu et al.*, 2010; *Kuhn et al.*, 1999; *Kesselmeier et al.*, 1999; *Maseyk et al.*, 2012], (2) field-based measurements of plant fluxes across ecosystems, and (3) boundary layer ambient surface measurements to address whether our understanding of the COS cycle is sufficient to close the gap between continental/seasonal variations [*Montzka et al.*, 2007; *Campbell et al.*, 2008] and the process scale [*Stimler et al.*, 2010a; *Seibt et al.*, 2010; *Sandoval-Soto et al.*, 2005].

A significant technical breakthrough toward addressing these issues is the ability to now make online COS measurements using infrared laser absorption spectrometry [*Stimler et al.*, 2010b]. This technique provides in situ measurement capabilities that historically were not possible using discrete flask and laboratory-based gas chromatography-mass spectrometry (GC-MS) analysis [*Montzka et al.*, 2007]. The results from *Stimler et al.* [2010b], *Asaf et al.* [2013], and [*Commane et al.*, 2013] all show measurements using this technique can be made at a temporal resolution greater than 1 Hz with an analytical uncertainty comparable to flask measurements. Here we take advantage of this new technology and (1) validate the critical assumption that the uptake ratio of COS to CO_2 is stable across a diversity of species and ecological settings and (2) evaluate the role that soils and entrainment play in controlling the boundary layer COS budget.

2. Methods

2.1. Analytical Instrument

The commercially available Los Gatos Research Inc. COS, CO_2, H_2O, and CO off-axis integrated cavity output spectroscopy analyzer (Model: 907-0028) was installed in a mobile trailer (Figure 1) [*Provencal et al.*,
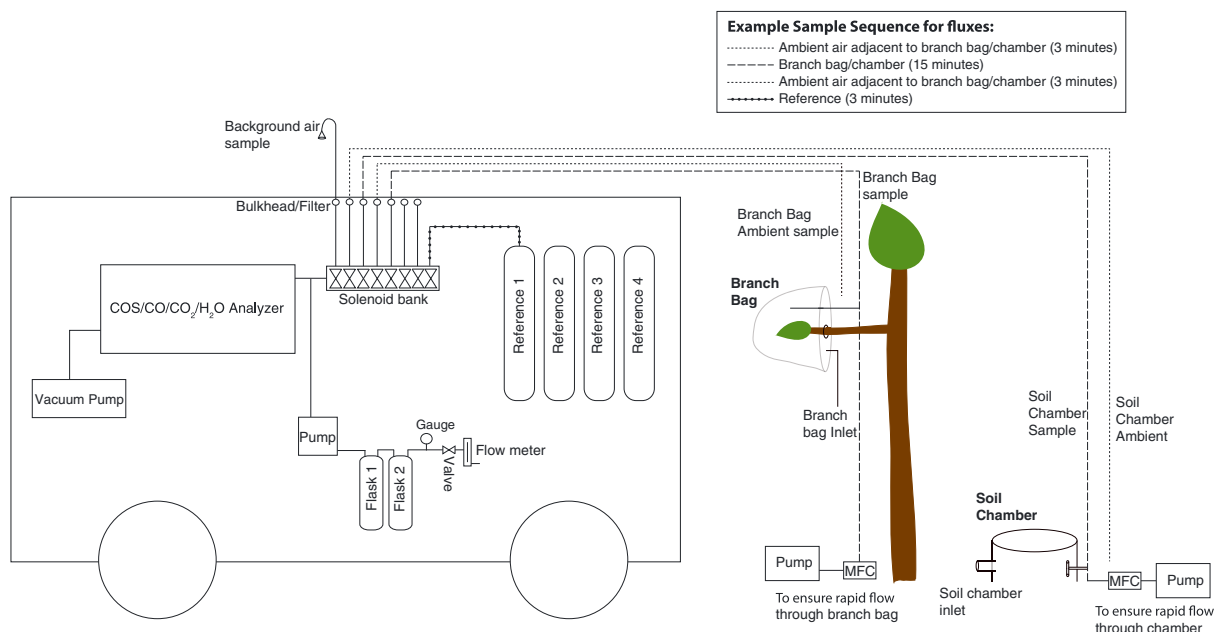
Figure 1. Schematic of the complete analytical setup for the campaign. See section 2 for details on instrument model specifications. The soil chamber is a custom welded stainless steel chamber [*Miller et al.*, 1999] and branch bag is a custom-made Teflon bag suspended with a stainless steel inner cage [*Harley et al.*, 2003]. All external plumbing was done using one-fourth inch Synflex, except for the inlet line suspended above the trailer, which was one-fourth inch stainless steel. The method used for flux analysis is described in the top right of the figure.

2012]. The system uses a 4.5 μm quantum cascade laser coupled into a high-finesse 400 cm^3 optical cavity and light transmitted through the cavity is focused onto an amplified HgCdTe detector. COS is detected at ~2050.40 cm^{-1}, CO_2 at 2050.56 cm^{-1}, CO at ~2050.86 cm^{-1}, and H_2O at ~2050.66 cm^{-1}. The pressure broadening associated with changes in the concentration of water vapor in the samples are corrected for in the spectral analysis routine. Concentrations for each species are reported throughout the paper as a dry mole fraction following correction for the dilution effect of the water vapor concentration. The cavity is maintained at a pressure of 6.0 ±0.03 torr with a flow rate of 1 L/min. Laboratory experiments show the system has a precision for COS, CO_2, and CO of 10 pmol mol^{-1}, 0.2 μmol mol^{-1}, and 0.6 nmol mol^{-1} for 10 s averaged measurements, respectively (Figure S1 in the supporting information). We did not assess the uncertainty in the H_2O retrievals, and therefore, these values are only discussed in relative terms.

There is negligible interference between COS and CO_2 across a wide range of concentrations (Figure S2 in the supporting information) and the humidity dependence of the COS measurement after correction for pressure broadening across the range of humidities observed during this campaign is within the analytical uncertainty of the instrument (Figure S3 in the supporting information). Although humidity measurements were not pinned to an absolute scale, the relative variations in H_2O concentrations are sufficiently constrained to correct for the pressure-broadening effects. Over the range of humidities experienced in the field, the bias associated with the humidity-dependence of the retrieval was smaller than the atmospheric signal of interest, and we thus chose to not apply any humidity-bias correction. Reference and sample gases were introduced into the analyzer through the Los Gatos Research Inc. Multiport Inlet Unit, a computer-controlled bank of solenoids (Figure 1). Four ultralow humidity reference gases with COS concentrations ranging from 340 to 433 pmol mol^{-1} and CO_2 concentrations ranging from 392.5 to 395.9 μmol mol^{-1} were used throughout the experiment to assess instrument drift. Values for the COS concentrations in the reference tanks were established through comparison against a reference gas that was generated by controlled dilution of a COS stream produced by a permeation tube in a controlled oven (Vici Model 150 Dynacalibrator). The values established for the tanks through the permeation tube process were verified by measuring the tanks against an additional reference tank in the field, which was tied to the NOAA Global Monitoring Division (GMD) lab [*Montzka et al.*, 2007]. The values reported hereafter can therefore be directly compared against other published results through analysis of this known standard reference. Reference gases were introduced every hour for 5 min intervals during periods when continuous

ambient measurements were being made and introduced for 3 min before and after each soil chamber and branch bag analysis. In addition, a series of flask samples were collected in pairs from the same plumbing as the air being introduced into the analyzer and analyzed by GC-MS following the methods of *Montzka et al.* [2007] for comparison against the in situ measurements (Figure 1).

2.2. Gas Exchange

Air sample inlet lines were plumbed into the trailer through a one-fourth inch diameter bulkhead fitting with a 2μm stainless steel filter to remove dust. Plumbing was done with a combination of stainless steel and Synflex®. The flow-through soil chamber used in this study was an acid-washed stainless steel cylindrical chamber, which encompassed a soil surface area of 177 cm^2 (Figure 1). All parts of the chamber were made with stainless steel to avoid the possibility of COS emissions from plastics or other synthetic materials. A one-half diameter stainless steel tube extending ~1 inch from the chamber was used to allow ambient air into the chamber and a one-fourth inch diameter outlet was plumbed into the analyzer. Flow through the chamber was maintained precisely at 2 L/min to ensure rapid turnover of air in the chamber and minimize the likelihood of condensation. In addition, the outlet tube was split into a tee within the chamber to encourage turbulent flow (Figure 1). The design of the chamber follows that of *Miller et al.* [1999], which specifies the need for a wide diameter inlet and narrow outlet to minimize the development of a pressure gradient between the chamber and ambient atmosphere [*Xu et al.*, 2006]. Throughout the campaign, a series of experiments were conducted to assess emissions and/or uptake from the soil chamber by sealing the bottom with a Teflon bag. These experiments consistently showed no measurable COS or CO_2 emissions (or uptake) from the chamber.

During sampling of the soil fluxes, litter was generally removed from the sample area and the chamber was inserted ~2 cm into the soil with a mallet to provide a good seal. A small number of analyses on leaf litter fluxes were also conducted by placing litter in the chamber and sealing the bottom with a Teflon bag. Air temperature inside the chamber was monitored during the soil flux analysis using a thermocouple. Gas concentrations in the soil chamber were measured for 15 min periods and data from the last 5–10 min of the analysis (after steady state values had been reached) were averaged. Measurements of ambient air were done for 3 min before and after each chamber analysis directly adjacent to the chamber inlet ($C_{ambient}$ in equation (1)). The ambient air was averaged over the 6 min window (3 min before and 3 min after) yielding an average uncertainty of less then 9 pmol mol^{-1}. Each soil chamber analysis was done in duplicate or triplicate, to minimize the influence that high-frequency variability in the concentrations of the gas species near the ground surface have on equation (1). Following analysis of a soil site, the chamber was removed from the ground, cleaned, and reset in a new location following the method described above.

Leaf fluxes were measured using a custom-made Teflon branch bag gas exchange system with an inner stainless steel wire that maintained air space between the Teflon bag and the leaves. The design of the system closely follows that described by *Harley et al.* [2003]. Flow through the branch bag was maintained at 3.8 L/min using a mass flow controller (Porter MPC Series), which was plumbed downstream of the sample pathway to avoid emission from the mass flow controller (MFC). The MFC was used to ensure rapid turnover of the air in the branch bag, which otherwise would quickly become depleted in COS and CO_2 from leaf uptake and saturated with water vapor. Repeat blank measurements done throughout the campaign revealed that air passing through the branch bag was elevated in COS by 40 pmol mol^{-1} ± 8 pmol mol^{-1} relative to the ambient air (though no change in CO_2 was observed) (Figure S4 in the supporting information). We believe this emission came from a small amount of putty that was used to seal the space between the branch bag and the branch. The magnitude of the blank did not significantly vary during the campaign and therefore a fixed blank correction of 40 pmol mol^{-1} with an assumed constant error in this term of 8 pmol mol^{-1} based on the average of repeat measurements of blanks. Air temperatures inside the branch bag were monitored with a thermocouple; however, no formal analysis of the temperature dependence of the blank magnitude was done. The total uptake of COS was generally in a range between 180 and 240 pmol mol^{-1} and therefore was significantly larger than the magnitude of the blank.

Leaf and soil COS and CO_2 fluxes, F_C, were calculated using the following equation (negating pressure and temperature effects on other gas fluxes) where "flow" is the flow rate through the enclosure in mol s^{-1}, COS and CO_2 concentrations for "ambient," "chamber," and "blank" are measured in pmol mol^{-1} and μmol mol^{-1}, respectively, and converted to mol mol^{-1}, "area" is in m^2 (a constant for the soil chamber and calculation of

leaf area is discussed below) and the resulting fluxes are reported hereafter in pmol m^{-2} s^{-1} and µmol m^2 s^{-1} for the respective species:

$$F_C = \text{flow} * \left[C_{\text{ambient}} - \left(C_{\text{branch/chamber}} - C_{\text{blank}} \right) \right] / \text{area} \qquad (1)$$

Leaf area was measured by removing all the leaves in the branch bag following analysis, scanning the leaves, and calculating the leaf area using Adobe Photoshop® software. We did not explicitly measure the sunlit leaf area, which changed dynamically across sampling periods due to self shading by leaves within the chamber. As a consequence, an upper limit on area was calculated by using maximum CO_2 assimilation rates, based on gas exchange measurements [*Monson et al.*, 2002; *Baldocchi et al.*, 2001], and solving for the effective sunlit area. This resulted in effective sunlit leaf areas between 40% and 70% of the measured leaf area. We acknowledge this approach may overestimate the leaf fluxes and therefore may contribute to uncertainty in scaling up of leaf fluxes. However, this approach does not negate comparisons between COS and CO_2 fluxes from individual chamber experiments (as area is canceled out in COS/CO_2 flux ratio) and therefore our estimates of Leaf Relative Uptake (described below) are not influenced by the assumptions going into the effective leaf area estimates.

Following *Stimler et al.* [2010a] and *Campbell et al.* [2008], the uptake ratio of COS to CO_2, referred to hereafter as leaf relative uptake (LRU), is defined by the following equation where F is the flux for the different species (pmol m^{-2} s^{-1} and µmol m^{-2} s^{-1} for COS and CO_2, respectively) calculated following equation (1) and [C] is the ambient concentration (pmol mol^{-1} and µmol mol^{-1} for COS and CO_2, respectively) of the gas in the chamber:

$$LRU = \frac{F_{COS_{leaf}}}{[COS]} / \frac{F_{CO_{2leaf}}}{[CO_2]} \qquad (2)$$

We introduce a new term, soil relative uptake (SRU), which is the normalized ratio of COS uptake and CO_2 release from the soil. SRU is defined as follows:

$$SRU = \frac{F_{COS_{soil}}}{[COS]} / \frac{F_{CO_{2soil}}}{[CO_2]} \qquad (3)$$

2.3. Sites

Between 27 July and 6 August 2012 the system operated in a riparian zone along Boulder Creek in Boulder, CO (40.01°N,−105.25°W, 1624.0 m above sea level (asl)). The site (hereafter referred to as GH) is densely populated by typical riparian trees for the region including *populus*, *alnus*, and *quercus* as well as some exotic trees such as *malus* and *catalpa*. Along the creek, the soils tend to be fine grained and saturated with significant moss. Away from the creek, the soils were rocky, dry, and covered with a thin litter of leaves, which was removed prior to soil flux analysis. Leaf flux measurements were made on all species at the site at a height of between 1 and 2 m above the ground. Ambient air measurements at this site were made within the canopy at a height of ~3.5 m through a stainless steel inlet at the top of the trailer (Figure 1). While wind data necessary to quantitatively estimate the footprint size that influenced the intake air composition were not available, given the inlet height and the density of the canopy, we estimate the footprint is less than 50 m [*Baldocchi*, 1997]. A road is located nearby the inlet and the influence of morning traffic is clearly observable as a rapid rise in CO concentrations each morning near to 7:00 local time (Figure 2). The CO concentrations remain high throughout the day showing evidence of a consistent influence of anthropogenic emissions. Radiation data for this site were taken from a Kipp and Zonen CMP 3 Pyranometer made available as part of University of Colorado's Skywatch Program (Figure S5 in the supporting information).

Between 7 and 13 August 2012, the system operated at the NOAA Boulder Atmospheric Observatory (BAO) (40.05°N, 105.01°W, 1584 m asl), which is a dry grassland site dominated by *Agropyron cristatum* and *Bromus tectorum* that are largely senescent in August. The site is surrounded by a large region (many kilometers) of grasslands and agricultural fields, which were largely fallow during the campaign period. Sequential measurements of ambient air at 1, 3, and 5 m were made from a 10 m tower on the site for the first 3 days and measurements were made continuously for the remaining 4 days at 100 m above the surface using NOAA Global Monitoring Division's (GMD) Synflex® tubing installed on the 300 m tower at the site. Simultaneous flask measurements at 300 m were taken during three of these days and measured by GC-MS as part of GMD's regular sampling and are used to provide further validation of the in situ measurements. Soil flux measurements in undisturbed grass-free regions of the soil were made during the first 2 days of the campaign here. Radiation, wind, and sodar data for the site were made available through GMD's BAO public ftp
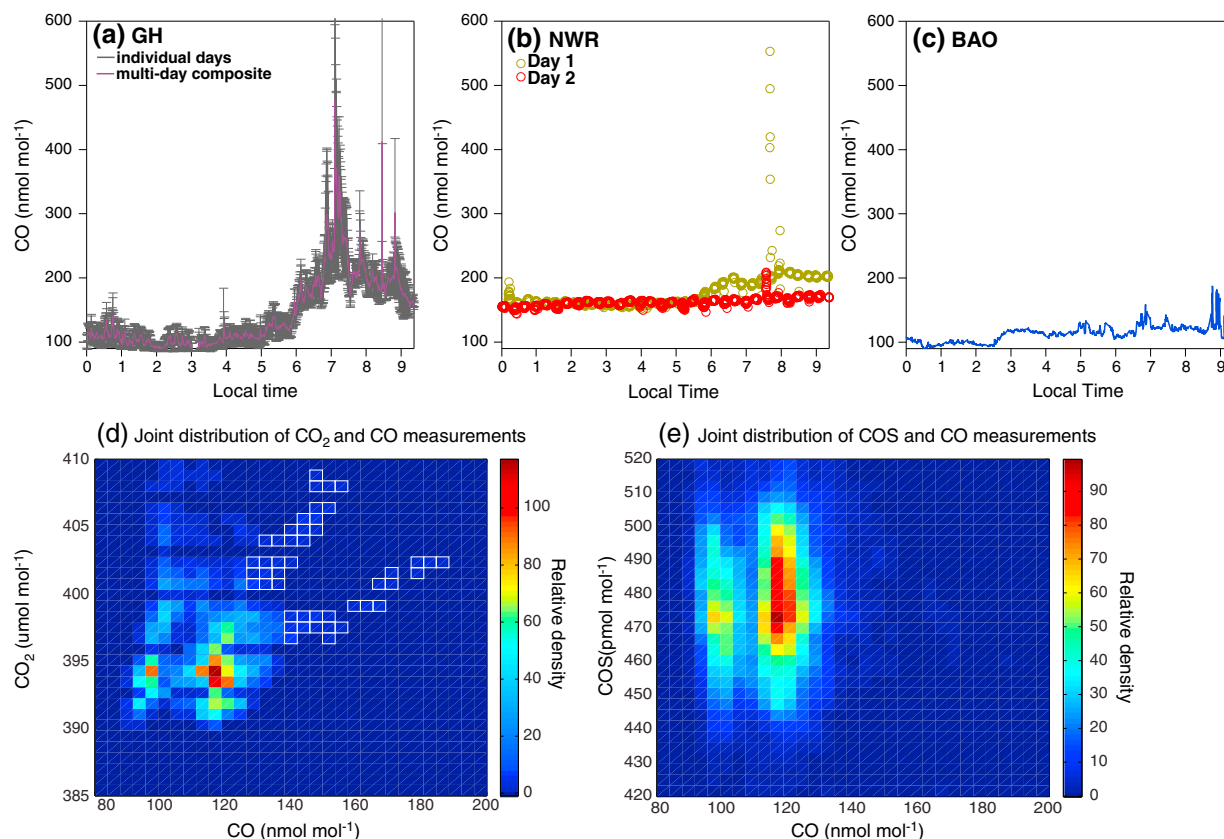
Figure 2. Nighttime to morning transition in the CO concentration of ambient air measured at the three sites. (a) The gray shows all the 30 s data for multiple days, while the red is the composite 30 s data for all the days. (b) The red and yellow dots are 30 s data from two separate days, the gaps arise from period when the branch bag and soil chamber were being measured. (c) The blue line is 30 s data from the surface at a single day at BAO. (d–e) The bivariate probability distribution between CO and CO_2 and CO and COS during 1 day at the GH site. Periodically, spikes in CO and CO_2 track one another. Because these events are rare and not well represented in the distribution, these values were highlighted by placing white squares around their location on the map. The presence of these features implies a common source of the two gases while COS is largely unresponsive to these temporary CO deviations.

site. No clear evidence of a morning CO spike was apparent at this site (Figure 2) reflecting its more rural setting relative to GH.

Between 13 and 18 August 2012 the system was moved to an alpine forest at the University of Colorado's Mountain Research Station, adjacent to the Niwot Ridge Long-Term Ecological Research site (40.03°N, −105.54°W, 2897 m asl). The site (hereafter NWR) was populated by *Pinus flexilis* and *Populus tremuloides* with a sandy dry soil that was covered by a thin (2–4 cm) litter. Ambient measurements were made within the canopy from a stainless steel inlet installed at a height of ~3.5 m, identical to the installation setup used at GH (Figure 1). This is an open canopy setting (LAI = ~4) with a primarily homogenous land surface in the sampling footprint. Leaf fluxes at this site were measured at heights of between 1 and 2 m in the canopy on trees of a similar age class. Soil fluxes were measured both with and without leaf litter present. The nearby area does not include any significant roads, and consequently, we do not observe a regular spike in morning CO as observed at GH (Figure 2). However, because we drove right up to the site, a small perturbation was present on one of the days from our own vehicle (Figure 2). Despite the lack of a regular morning transition in CO, the concentrations at this were consistently high and suggest a possible influence of biomass burning on the air at this site. Radiation and wind data from this site were taken from the AmeriFlux archives (site: NWT) operated nearby to the sampling trailer (Figure S5 in the supporting information).

3. Results and Discussion
3.1. Instrument Performance
Field measurements of COS using laser absorption spectrometry is still a fledgling technique [*Asaf et al.*, 2013; *Commane et al.*, 2013], and therefore, an objective of this study was to quantitatively assess the
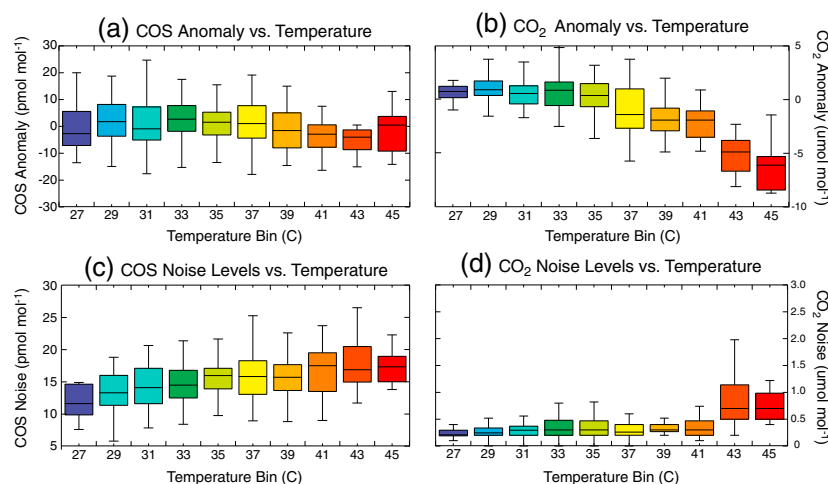
Figure 3. (a) COS reference gas anomalies from throughout the campaign binned in 2°C windows. (b) CO_2 reference gas anomalies from throughout the campaign binned in 2°C windows. (c) Distribution of the standard deviation of 3 min windows of 1 Hz COS data when reference gas was being introduced throughout the campaign. (d) Distribution of the standard deviation of 3 min windows of 1 Hz CO_2 data when reference gas was being introduced throughout the campaign. All box and whisker plots show the 5, 25, median, 75, and 95% quartiles.

performance of a commercially available instrument in a difficult field environment. By continually introducing a reference gas under normal field conditions, we determined an operational uncertainty of ≤10 pmol mol^{-1} and 2 μmol mol^{-1} for COS and CO_2, respectively, when an averaging window of ≥30 s was applied to the 1 Hz measurements (Figure S6 in the supporting information). The uncertainty from the field measurements is larger than that obtained in the lab (Figure S1 in the supporting information), which is likely a consequence of the lack of instrument temperature control in the field. We assume the uncertainty arising from the field experiments to be the appropriate values for the data presented here. Unless otherwise stated, a 30 s averaging window was applied to the data. There was a strong temperature dependence in the CO_2 concentrations, measured as the temperature of the gas entering the optical cavity. The inlet lines were not insulated and there was no temperature control in the trailer, which yielded large fluctuations in the gas and instrument temperatures, respectively. The effect was characterized and all CO_2 measurements were corrected accordingly yielding an operational uncertainty of ≤1 μmol mol^{-1} for 30 s averages (Figure S6 in the supporting information). A similar temperature dependence was not observed for the COS measurements, though both species show an increase in uncertainty at high instrument temperatures (Figure 3 and Figure S7 in the supporting information). The upper temperature limit for reliable measurements with this instrument is ~45°C and the field conditions did not permit an assessment of a lower temperature limit.

The COS concentrations were tied to an absolute concentration scale by frequent measurements of the four reference gases. The concentrations of these gases were established through calibration against a diluted COS stream produced by a controlled process using a permeation oven in the laboratory and validated by measurement against a reference gas tied to the NOAA GMD lab. Using these four known points, a linear equation of the form, $COS_{actual} = m*(COS_{measured}) + b$ was applied to the raw data ($b = -43.0$ pmol mol^{-1} and $m = 1.1$). Following application of this correction to all data, the influence of instrument drift was corrected using the individual calibration points measured throughout the experiment. It was noted that when the calibration gas in the reference tanks dropped below pressures of 6895 Pa, significant outgassing of COS began to influence the stability of the reference gas and consequently these tanks were removed from the calibration rotation.

After correcting the COS measurements to absolute concentrations, tied to a NOAA-GMD standard using the span of reference gases, a mean offset between the flasks (collected simultaneously with the analyzer and measured at NOAA GMD using GC-MS) and the laser analyzer of 4 pmol mol^{-1} was observed. This was based on three pairs of flasks and coincident 30 min averaged windows from the analyzer. The difference is within the precision of the spectrometric measurements, providing comparison of spectrometric and chromatographic-independent calibrations. Using both the four span reference gases and the comparison
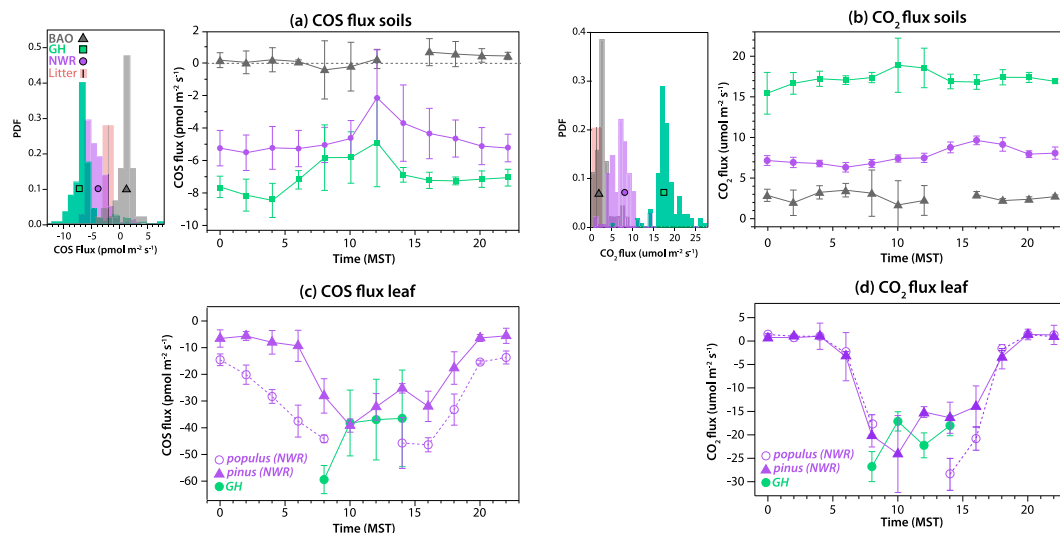
Figure 4. (a) Distribution (left) and diel time series (right) of the COS flux from the soils at the three sites. The litter flux was only measured at the NWR sites, and there were insufficient measurements to produce a meaningful distribution. (b) Distribution (left) and diel time series (right) of the CO_2 flux from the soils at the three sites. Note that negative values capture removal/uptake of COS from the air. (c) COS flux from the branch bag experiments. These data were only collected at the GH and NWR sites, and nighttime data were only measured at NWR; thus, the diel cycle is based on data gathered from that site only. The data at NWR were split into broad leaf *Populus tremuloides* and coniferous *Pinus ponderosa*, and all the species (listed in Table 1) were averaged together at the GH site. (d) CO_2 flux from the branch bag experiments. Nighttime measurements were only done at NWR. Error bars on all diel plots show 1 standard deviation of error based on all the data that fell into the 2 h bin.

against the flask measurements, we find a linear response of the instrument from 340 to 500 pmol mol^{-1}, and we assume this response applies to the entire range of measurements (240–590 pmol mol^{-1}). This assumption is further validated by comparison between the 100 m in situ and 300 m NOAA GMD GC-MS flask measurements at the BAO site (discussed in section 3.4.2 and shown in Figure 8), which were taken when COS concentrations were close to 550 pmol mol^{-1} (and 390 μmol mol^{-1} for CO_2).

3.2. Leaf Fluxes
3.2.1. Greenhouse Site
At the GH site, measurements from 10 genera of trees within the canopy yielded an average uptake flux across species of −45 pmol m^{-2} s^{-1} (±15 pmol m^{-2} s^{-1}) (Figures 4 and 5). Because only coarse estimates of sunlit area were made and sampling was done for different species at different times of day, we do not make any quantitative comparisons of assimilation rates across genera though, in general, find the largest uptake fluxes from broad-leafed trees. The magnitude of the COS fluxes correlate with a high degree of significance against H_2O fluxes (Figure 5), implying a strong stomatal control of COS uptake [*Stimler et al.*, 2010a]. During the night when conductance is very low and the air approaches saturation, the relationship between H_2O and COS fluxes weaken (Figure 5, bottom left points). The COS and CO_2 fluxes also strongly covary, with an average LRU (equation (2)) across species of 2.1 (± 1.1) (Table 1). The average LRU drops to 1.8 (± 0.7) if the outlying value of 4.9 derived from the *Populus fremontii* samples, which was measured when ambient temperatures in the branch bag were ≥40°C, is excluded. The joint COS and H_2O fluxes from the *Populus fremontii* samples fall significantly off the curve defined by the other species, while the joint CO_2 and H_2O fluxes fall on the curve set by the other species (Figure 5). This suggests an oddity to these measurements and warrants their exclusion from being averaged with the other LRU values. One possible explanation is that these data could be the result of condensation within the branch bag or sample line that adversely affected the COS flux estimates or, alternatively, that a nonleaf component of the plant (i.e., a bud) was taking up COS, while neither transpiring H_2O nor taking up CO_2.
3.2.2. Niwot Ridge
The branch bag experiments at NWR yielded COS fluxes with a daytime (9–17:00 local time) average of −36 pmol m^{-2} s^{-1} (±8 pmol m^{-2} s^{-1}) (Figure 4). A higher average COS flux was observed for the broad-leafed *Populus tremuloides* (−45 pmol m^{-2} s^{-1}) than the coniferous *Pinus flexilis* (−32 pmol m^{-2} s^{-1}).
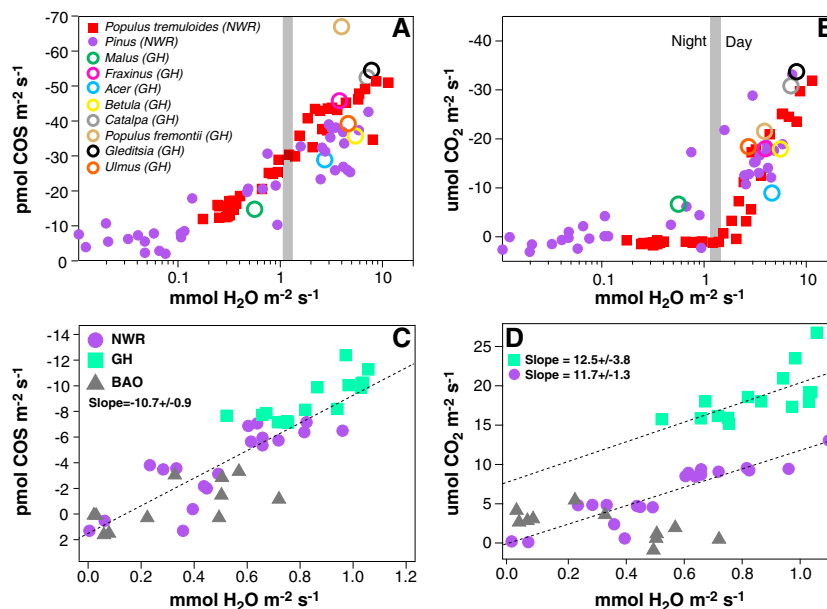
Figure 5. (a) COS versus H_2O fluxes for the branch bag experiments at the GH (open circles) and NWR sites. *Y* axis is reversed to emphasize the relationship between transpiration and COS uptake. (b) Same as Figure 5a except for CO_2 instead of COS. The gray bar denotes the approximate transition between daytime and nighttime measurements. As can be seen, the COS uptake remains linearly related to H_2O across this transition, whereas CO_2 asymptotes near 0 across this boundary. (c) COS versus H_2O fluxes for all soil chambers at the three sites. To minimize the impact of temperature, only soil chamber instances in a narrow-temperature window (33–36°C for NWR, 36–39° for BAO, and 42–45° for GH) were used. The dotted line is the linear regression through all the data. (d) Same as Figure 5c except for CO_2. The upper dotted line is the best fit through GH and the lower dotted line is the best fit through NWR. There is no significant linear response between the two variables at BAO.

The joint COS and H_2O fluxes fall approximately along the same curve as fit to the GH data, though the campaign at this site included nocturnal measurements (discussed below) and therefore capture a wider spectrum of the curve (Figure 5). The average of all branch bag measurements between 9 and 17:00 yielded an LRU value at NWR of 1.6 (Table 1) with no statistically significant difference between the coniferous and broad-leafed trees. While LRU is stable during daytime hours, its value becomes unstable at night when the denominator of equation (2) (CO_2 flux) approaches 0 and reverses sign (Figure S8 in the supporting information). Therefore, we include no further discussion of the nighttime LRU values.

Unlike CO_2, where light is required for assimilation, COS consumption by carbonic anhydrase continues at night as long as there are open stomata [*Protoschill-Krebs et al.*, 1996; *Simmons et al.*, 1999]. Nighttime

Table 1. Normalized Leaf Relative Uptake Values Across the Campaign

Genus (Species)	Mean	Median	*n*	Hour of Day	Temperature (C)	Site
Malus sp.	2.1	2.1	2	12.2	37.9	GH
Fraxinus sp.	1.6	1.5	4	14.7	38.0	GH
Acer sp.	2.3	2.3	2	10.6	33.0	GH
Catalpa sp.	1.7	1.7	5	13.5	39.4	GH
Betula sp.	1.6	1.5	3	15.2	38.8	GH
Populus fremontii	**4.9**	4.9	3	15.8	40.9	GH
Ulmus sp.	1.9	1.8	3	11.2	34.3	GH
Gleditsia sp.	1.4	1.4	2	11.8	35.1	GH
Pinus ponderosa	1.3	1.4	3	12.7	NaN	GH
Quercus sp.	1.5	1.6	4	10.8	NaN	GH
Populus tremuloides	1.6	1.6	19	13.5	32.5	NWR
Pinus flexillis	1.5	1.4	15	12.1	29.9	NWR
All Samples[a]	**1.7**	**1.6**	65	-	-	-

[a]Daytime (9:00-17:00 local time) LRU (unitless) for all measured tree genera. Excluding *Populus fremontii*. Bold numbers denote the outlying value of *Populus fremontii* and the average (mean and median) LRU that emerges from all measurements.

measurements of the joint COS and H_2O fluxes reveal the stomatal control of COS uptake by showing that the nocturnal and diurnal fluxes fall along the same curve except in the cases of extremely low conductance (Figure 5). The diel structure of COS and CO_2 fluxes therefore differ significantly as CO_2 assimilation sharply begins each day near to 6:00 and ends near to 18:00, in correspondence with the daily cycle in downward shortwave radiation (Figure S5 in the supporting information). The nocturnal conductance and uptake of COS is significantly larger for the broad-leafed species (10–30 pmol m^{-2} s^{-1}) than the coniferous species (6–9 pmol m^{-2} s^{-1}) (Figures 4 and 5). An intriguing feature of the uptake of COS by *Populus tremuloides* is that it reaches a minimum near to midnight and then begins to increase as dawn approaches. The opening of stomata after prolonged darkness has been noted in other species [*Caird et al.*, 2007] and may represent an adaptation by plants to "anticipate" sunlight [*Heath*, 1984]. The incomplete stomatal closure and higher stomatal density in the broad-leafed aspen species results in instantaneous nocturnal uptake of COS that can be as much as 25–30% of average daytime fluxes.

3.3. Soil Fluxes
3.3.1. Greenhouse Site
At the GH site, the soils had a daily average COS uptake flux of −7.0 pmol m^{-2} s^{-1} ±2.6 pmol m^{-2} s^{-1}, based on 107 chamber measurements (Figure 4). The largest fluxes of $\sim$ −11.0 pmol m^{-2} s^{-1} were observed in the damp soils dense with roots nearer the creek during the warmest period of the day (Figure S9 in the supporting information). Three of the 107 instances showed COS emissions, two of which also occurred when ambient and soil chamber temperatures were ≥35°C (Figure 4 and Figure S9 in the supporting information). The magnitude of the COS flux exhibited a statistically significant negative correlation with background COS values suggesting that the rate of uptake is driven in part by the ambient to soil-air concentration gradient (Figure S9). However, a number of points deviate significantly from this curve indicating the presence of multiple competing processes impacting the magnitude of the soil flux.

While no explicit measurements of soil moisture were made, H_2O fluxes from the soil chamber measurements were used to elucidate some information on soil moisture controls on COS flux. By comparing COS and H_2O fluxes taken within a narrow temperature range (3°C window at each site), the influence of temperature on soil water flux is minimized and the residual variability is assumed to relate to changes in the soil moisture. We find a significant negative correlation between H_2O and COS fluxes from the soil and a positive relationship between H_2O and CO_2 fluxes (Figure 5). The response of the COS flux to soil moisture is generally consistent with the findings of *Kesselmeier et al.* [1999], though the lack of an obvious temperature control on COS flux deviates from previous work (Figure 4 and Figure S9 in the supporting information). This may be the result of the fact that temperatures were measured in the air space above the soil as opposed to within the soil itself. Nonetheless, the magnitudes of the COS and CO_2 fluxes were significantly negatively correlated with one another such that soils with the highest respiration rates were also those with the greatest COS uptake. This largely reflects that respiration is associated with carbonic anhydrase activity and both processes are influenced by moisture, temperature, and porosity [*Berry et al.*, 2013]. The average soil relative uptake (SRU) (equation (3)) for this site is −0.76±0.11, which varied minimally between the different soils measured and was stable across the temperatures observed at this site (26–45°C) (Figure 6).

3.3.2. Niwot Ridge
At NWR, the soils exhibited an average COS flux of −4.9 pmol m^{-2} s^{-1} ±1.8 pmol m^{-2} s^{-1} based on 135 measurements (Figure 4). The fluxes at this site were typically smaller than at GH and exhibited less variability, which reflects a more homogenous environment (dry alpine site with two dominant tree species). Of the 135 measurements, four chamber measurements showed emissions which were clustered at times when the chamber air temperature was ~35°C, similar to that observed at GH. As with GH, the largest uptake occurred during the warmest period of the day though otherwise no systematic correlation with temperature was observed (Figure S9 in the supporting information). COS uptake at this site was significantly correlated with background ambient COS concentrations as at GH (Figure S9 in the supporting information). The similarity in the slope between the uptake flux and the ambient COS concentrations suggests, despite a lack of characterization of the physical properties of the soils (e.g., porosity), that diffusion rates of COS into the soils were fairly constant. Soil flux measurements made with litter in place produced soil fluxes that were smaller (−2.1 ± 0.2 pmol m^{-2} s^{-1}) than adjacent soil plots without litter (−4.4 ± 0.6 pmol m^{-2} s^{-1}). The flux of litter isolated from the soil yielded a flux nearly identical to that of the soil with litter in place (−2.04 ± 0.4 pmol m^{-2} s^{-1}) (Figure 4). Some initial hypotheses to explain the influence that litter had on soil COS uptake are that it acts to reduce the concentration of COS at the soil surface below and thus reduces the gradient and/or that litter limits the efficiency for air to penetrate into soil pore spaces.
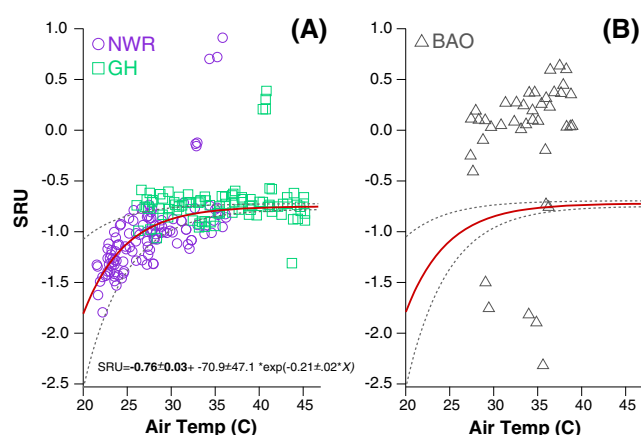
Figure 6. Soil relative uptake (equation (3)) at (a) NWR and GH and (b) BAO as a function of the soil chamber air temperature. The best fit exponential regression for GH and NWR is shown in red with the gray dotted lines showing the 95% confidence intervals from a bootstrap analysis. One standard deviation errors in the coefficients of the equation based on the bootstrap regression are also shown in the figure. The same regression line is shown in Figure 6b for comparison between the NWR/GH and BAO sites.

H_2O and COS fluxes from soils within a narrow temperature range significantly correlated against one another, indicating a similar response between the NWR and GH soils to moisture (Figure 5). While there is some indication of a diel cycle in soil fluxes, COS fluxes diverge at high temperatures showing both the highest and lowest uptakes during the middle of the day (Figure 4). There was a significant and negative correlation between COS and CO_2 fluxes with an average SRU value of -1.08 ± 0.22 (Figure 6). SRU values exhibited a strong sensitivity to air temperature such that at low temperatures, the values drop rapidly. When SRU values from both NWR and GH are taken together, the two converge on a common value of -0.76 at temperatures $\geq 26°C$. Treating SRU as a function of soil chamber air temperature, an exponential regression provides a sufficient empirical model to account for most of the influence of temperature on SRU (Figure 6). Although not explicitly shown, the temperature dependence of SRU results in a diel cycle in this property.

To a first order, the physical significance of the temperature dependence of SRU arises as a consequence of the fact that the physiological controls on both CO_2 and COS fluxes are sensitive to temperature [*Berry et al.*, 2013]. For both gases, this response is nonlinear [*Kesselmeier et al.*, 1999; *Qi et al.*, 2002], with CO_2 respiration rates from soils rising exponentially with temperature (when sufficient substrate is accessible) and the rate of COS consumption by soil carbonic anhydrase having a parabolic shape with a maximum uptake occurring at ~20°C [*Kesselmeier et al.*, 1999]. Ambient COS concentrations also vary significantly throughout the day following air temperature (as discussed in section 3.4.1 and Figure 7), indicating a second mechanism to influence the rate of consumption/emission that would follow (though not causally) ambient temperature. A theoretical explanation of the drop in SRU below 26°C arises from the fact that COS uptake is approaching its maxima, while CO_2 flux is less responsive to temperature changes in this range. There are, however, some rather surprising elements of the shape of this function at higher temperatures. It would be predicted from previous work that COS uptake would ultimately diminish at high temperatures, while CO_2 fluxes would continue to rise. This behavior would not give rise to an SRU asymptote but rather values that would continue to rise to positive numbers if net emissions began to occur. The absence of this relationship coupled to the fact that CO_2 fluxes exhibited a muted diel cycle (Figure 4) implies that the measured surface temperatures are not likely representative of the temperatures where CO_2 respiration and CA reactions with COS are actually taking place. Rather, we assume these reactions are occurring at depths below the surface that are cooler and have a lower amplitude diel cycle that lags air temperature.

3.3.3. Relationship Between Leaf and Soil Fluxes

In considering the soil fluxes relative to the leaf fluxes, SRU is opposite in sign and a factor of two smaller than LRU. Therefore, soil enhances an ecosystem's COS uptake, while reducing net CO_2 uptake. In order to directly compare the fluxes of soil and leaves on the ecosystem scale (~7 pmol m^{-2} s^{-1} and 40 pmol m^{-2} s^{-1}, respectively) the two values must be scaled taking into account the leaf area index (LAI). Using LAI values of 4.2 and 8 for NWR and GH [*Monson et al.*, 2002; *Nagler et al.*, 2004] and making no assumption about the distribution of broad to coniferous species (i.e., using a simple average leaf flux from all measurements), we report that at the ecosystem scale, the daytime (9–17:00) COS flux from soil is between 2 and 6% of that from plants. At night, the uptake of COS by soil and plants are similar to one another though the ratio of soil to leaf flux at night would be very sensitive to the distribution of broad leafed to coniferous species (the former having significantly higher nocturnal conductances).
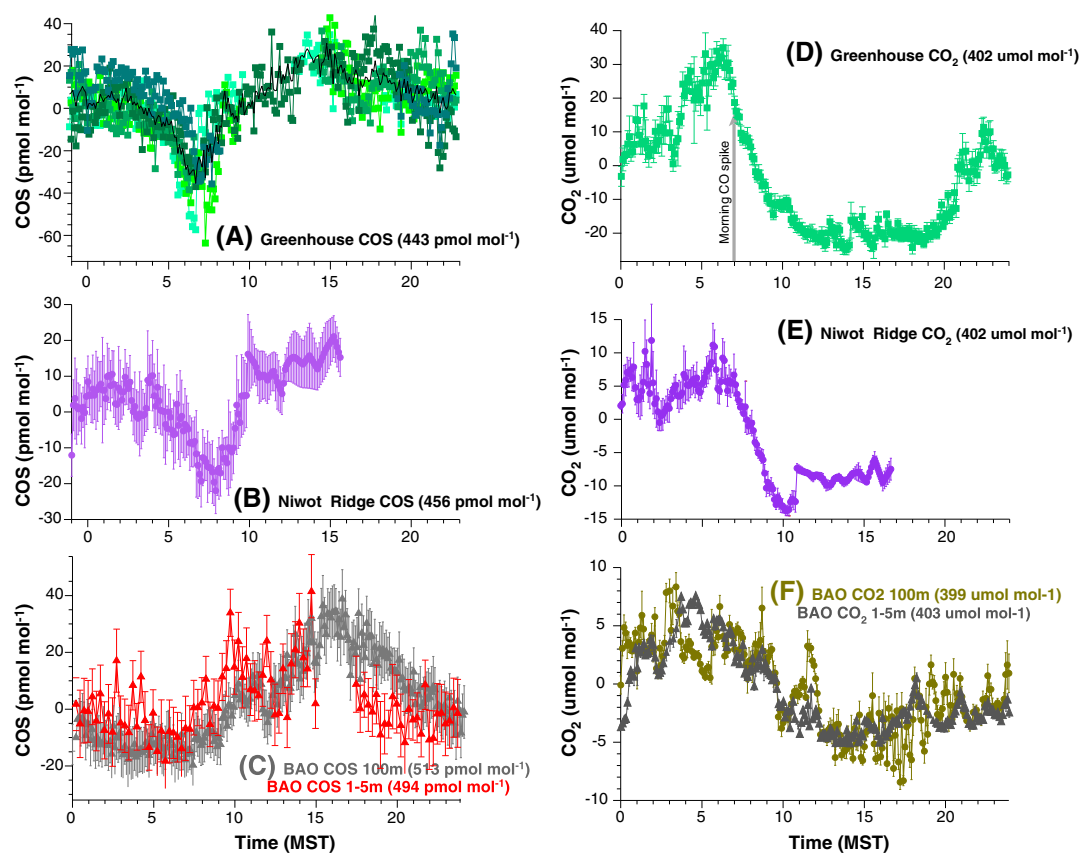
Figure 7. The diel time series in the ambient (a–c) COS anomalies and (d–f) CO_2 at the three sites. The mean value subtracted from each time series to generate the anomalies is specified in parenthesis next to the label. At GH, each of the lines shows the results from the different days, while the black lines show the composite average. At the other sites, the diel cycle was composited from sections of different days (i.e., there are not continuous diel cycles from different days), and therefore, we represent the composited time series with a 1 standard deviation error bar. The red line in the BAO plot shows the surface/3 m data, while the gray line is air sampled from the NOAA GMD 100 m intake line on the tower. Figures 7d–7f are the same as left column except for CO_2 concentrations.

3.3.4. Boulder Atmospheric Observatory

At the BAO site, the COS flux from soils (measured in bare areas between grassy patches) was +0.05 pmol m^{-2} s^{-1} ±1.8 pmol m^{-2} s^{-1} based on 44 soil chamber measurements taken over the course of 2 days (Figure 4). During chamber measurements where COS uptake was recorded, the magnitude of the COS flux was negatively correlated with ambient COS concentrations along a slope similar (though steeper) to what was observed at GH and NWR (Figure S9 in the supporting information). During chamber measurements when COS emissions were observed, this relationship is reversed such that the COS flux tracks ambient COS concentrations. The direction (emission versus uptake) and magnitude of the COS flux loosely follows surface temperature where measurements taken above 40°C primarily resulted in COS emissions (Figure S9 in the supporting information). The soils at BAO were generally more desiccated than at the other sites based both on the magnitude of the H_2O fluxes from these soils (Figure 5) and observations of a dusty surface. There is not a significant linear response of COS to H_2O fluxes at this site though the data cluster roughly along the line formed by the other two sites. The data from the three sites collectively suggest the possible presence of a moisture threshold at which point the soil begins to behave as an emitter though in this data set the emission fluxes remain close to zero in all instances (Figure 5).

The mean SRU at BAO is 0.08 and displays a relationship with temperature that is opposite in sign (positive) and form (linear) relative to the relationship observed at the other two sites (Figure 6). The difference in the response of SRU to temperature at this site may, in part, reflect the fact that soil and ambient temperatures at an open site (i.e., BAO) follow one another, while in a shaded canopy (as at GH and NWR) there are longer lags as a consequence of more diffuse radiation. However, the fact that CO_2 and COS emissions correlate
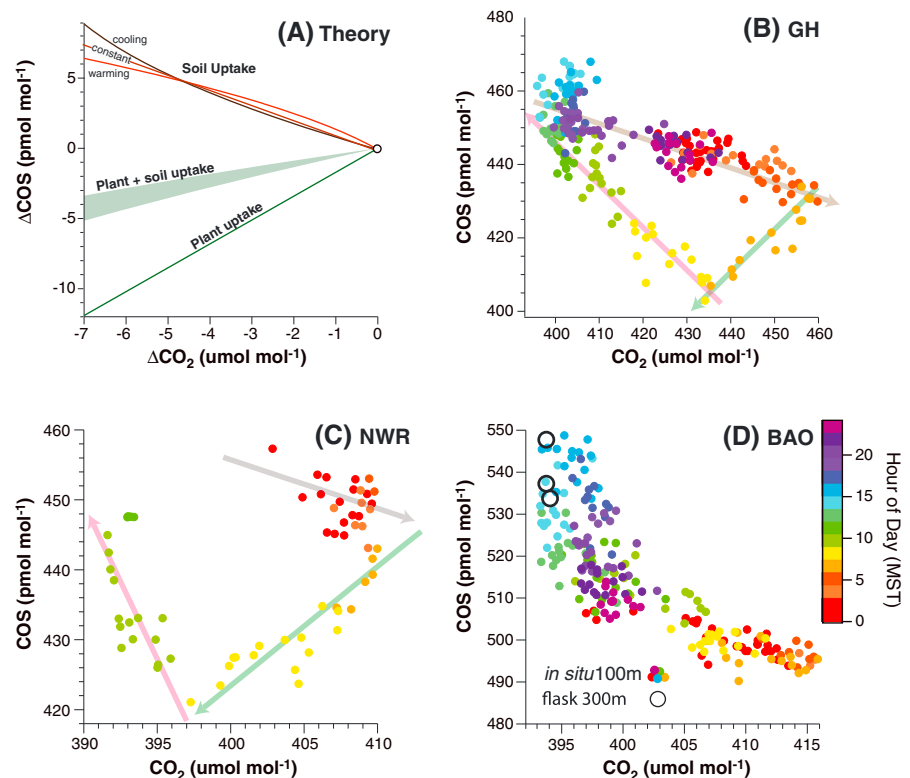
Figure 8. (a) Lines representing the trajectory of an air mass in COS-CO_2 space assuming the only process acting on air is vegetation (green) and soil (red/brown). Because SRU is temperature sensitive, the trajectory of soil uptake varies under different temperature regimes. Examples are shown for a soil "cooling" from 40 to 20° and "warming" from 20 to 40°. A mixture of soil and leaf processes is shown as a green wedge. The units are Δ reflecting an anomaly from an arbitrary starting concentration. (b–d) Scatterplots showing the covariation of COS and CO_2 at the three sites. The markers are color coded by the hour of the day. The lines highlight the three periods of the days dominated by plant uptake (green), entrainment (red), and soil/plant (brown). The white circles in Figure 8d are from flasks filled at 300 m and measured at NOAA GMD by GC-MS.

positively with each other implies the presence of an alternative mechanism to link these fluxes. As suggested by *Maseyk et al.* [2012], senescent vegetation acts as a COS emitter, and therefore, the presence of a positive relationship between COS and CO_2 fluxes, that is not observed at the other sites, may be the result of emissions of both gases from dead and decaying vegetation in the soil. However, as noted above, aspen and pine litter measured at NWR did not produce measurable COS emissions.

3.4. Ambient Measurements
3.4.1. Greenhouse and Niwot Ridge
The diel cycle in the ambient air sampled at ~3.5 m above the surface at GH is characterized by a drop in COS concentrations of ~10 pmol mol^{-1} between 4 and 6:00 MST followed by a steep decline of ~30 pmol mol^{-1} between 6 and 8:00 MST (Figure 7) that begins coincident with sunrise (Figure S5 in the supporting information). The concentration rises from the morning minima at 8–9:00 of 400 pmol mol^{-1} to a midday maxima of 470 pmol mol^{-1} by 16:00 MST (Figures 7 and 8). By contrast, CO_2 concentrations are characterized by a steady rise though the night of ~40 µmol mol^{-1} to ~440 µmol mol^{-1} followed by a sharp decline in the morning to values of 395 µmol mol^{-1}, where the concentrations remain relatively stable through the day (Figure 7). At NWR, the ambient air, also measured at ~3.5m, follows the same general diel pattern with COS concentrations dropping 30 pmol mol^{-1} between 5 and 9:00 MST followed by a steep rise to concentrations of 450–460 pmol mol^{-1} (Figures 7 and 8). CO_2 concentrations at this site rise by ~30 µmol mol^{-1} during the night and rapidly drop to values of 393 µmol mol^{-1} by midday.

The time-dependent covariation between COS and CO_2 at the surface arises as the sum of competing and interacting processes including (1) fluxes from the soil (uptake of COS and respiration of CO_2), (2) uptake of

COS and CO_2 by plants, (3) changes in the boundary layer height and entrainment of air from above, which generally drives COS concentrations up and CO_2 concentrations down, and (4) changes in wind speed and direction, which influence the sources and sinks of the gas species in the footprint. At both GH and NWR, variations in the relative influences of these processes results in the approximately triangular trajectory in Figure 8. Beginning at sunrise, there is a brief period in the morning (∼6–9:00 MST), when the two species fall along a positive line with a slope of 1.2–1.8. This transitional period occurs prior to significant growth of the boundary layer as evidenced by sodar data from the BAO site (Figure S10 in the supporting information). The fact that the slope between the gases is positive and close to the ratio of the fluxes associated with plant uptake (i.e., LRU) suggests that during this brief period in the morning, plant uptake exerts the dominant influence on the rate of change of the boundary layer concentrations of COS and CO_2.

There are other possible mechanisms to explain the covariation of these gases during this period including entrainment of residual air that had previously experienced photosynthesis or a change in wind direction or speed that influenced the footprint of the measurement. As discussed, this transitional period in the morning occurs prior to rapid boundary layer growth as seen in the sodar data and therefore seems unlikely that significant entrainment of an air mass is driving the strong variations in surface concentrations of COS and CO_2. This feature emerges at both NWR and GH, which have distinct impacts from anthropogenic emissions (i.e., car exhaust) (Figure 2) and was observed on multiple days experiencing different wind regimes (Figure S11 in the supporting information). These observations strongly support the interpretation that this feature is driven by a local boundary layer process associated with uptake by plants. In another study from a nearby open canopy forest in Colorado, *Berkelhammer et al.* [2013] used a set of isotopic tracers (δD and δ^{18}O) to evaluate water fluxes from plants and noted a similar transitional period in the morning when transpiration from plants left a strong isotopic anomaly on the vapor in the canopy air. This signature was quickly erased by 9:00 following the onset of entrainment, bearing a close resemblance to the observations presented here. The fact that the slope during this period is slightly shallower than what would be predicted from vegetation uptake alone may arise both from the impact of soils on the COS and CO_2 surface budgets and from small amounts of mixing with air above the boundary layer (Figure 8).

As the day progresses (9–15:00 MST), the slope between the two species is reversed, which could arise from either entrainment of residual boundary layer air which contains high concentrations of COS and low concentrations of CO_2, a shift between westerly (downslope) and easterly (upslope) flows or soil fluxes [*Kuhn et al.*, 1999] (Figure 8). The presence of a negative slope between these species negates the possibility that plant uptake is solely responsible for the observed variations in surface COS and CO_2 concentrations during this time (Figure 7). Entrainment is likely the dominant process influencing the surface concentration based on the observations that (1) the initial change in slope is coincident with rapid growth of the boundary layer (Figure S10 in the supporting information), (2) the same pattern emerges on days with both strong and negligible downslope-upslope flow transitions (Figure S11 in the supporting information), and (3) that the soil fluxes are too small to account for the observed changes in surface concentrations (Figure 4).

The concentration of COS in the air mixed down into the canopy from above will vary on synoptic time scales associated with shifts in the predominant wind direction and changes in the magnitude of the sources or sinks along the trajectory of the air parcel [*Campbell et al.*, 2008]. The consistency in the structure (amplitude and timing) of the diel cycle between days implies variability in the concentrations of these gases in the above canopy air is small relative to the boundary layer processes impacting the surface concentrations. In coastal regions where shifts between easterly and westerly flow will change whether an air parcel is passing over a COS sink or source [*Commane et al.*, 2013], such wind shifts would produce large variations in the influence that entrainment has on the surface concentrations. However, because of both the small footprint of the measurements and that the region is vegetated in all directions, transitions in the easterly and westerly flow appear to produce only a relatively subtle shift in gas concentrations.

After the sun sets (Figure S5 in the supporting information) and the land surface begins to cool (∼19:00), the slope between COS and CO_2 remains negative but with a shallower slope (∼ −0.6) than observed during the day. During the evening, plants and soil continue to uptake COS while emitting CO_2. These processes alone could account for covariation between COS and CO_2 at night. Some mixing of air into the canopy during the night could also be playing a role in the observed trends, though better characterization of nighttime stability would be needed to constrain the relative influence of these processes.
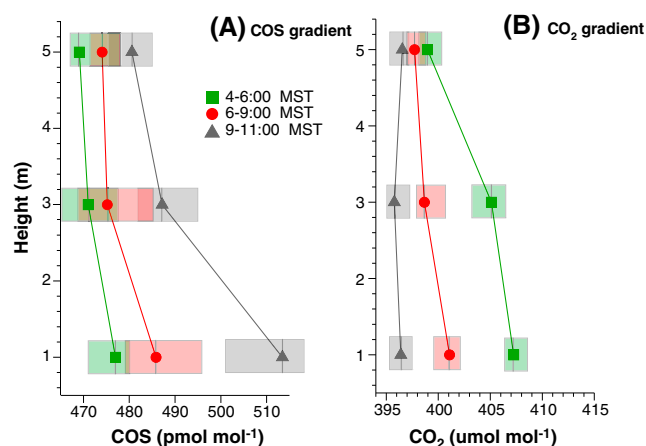
Figure 9. (a) Vertical gradients in COS from 1 to 5 m at BAO during three windows of the day. Boxes show the 25–75% quartiles. The increase ins surface values as the day proceeds is interpreted to reflect the presence of a surface source, which is controlled by temperature or radiation. (b) Same as Figure 9a except showing CO_2. Near-surface nighttime CO_2 values are greatest due to soil respiration but rigorous mixing of low CO_2 air during the day relieves this gradient.

3.4.2. Boulder Atmospheric Observatory

The diel cycles in COS concentrations both near the surface and at 100 m at the BAO are clearly distinct from the trends observed at GH and NWR (Figures 7 and 8). At BAO, the COS concentrations in the nighttime air are significantly higher than those observed at the other sites though comparable to the concentrations observed during the midday maxima at the other sites (460–470 pmol mol^{-1}). Some of the differences between the nighttime BAO concentrations and those observed at the other sites is that during the evenings, the 100 m inlet is generally above the boundary layer, while inlets at the other sites were sampling air from within the boundary layer (Figure S10 in the supporting information). However, the similarity in the COS concentrations at the surface and 100 m

at BAO (i.e., within and above the boundary layer) indicate the enriched nighttime concentrations relative to the other sites does not simply arise from differences in the sampling height. The absence of a vertical gradient during the evenings implies that there is minimal surface COS exchange (Figure 7). We hypothesize that significant uptake of COS by soils and plants during the night with the addition of a lack of turbulent mixing would generate strong vertical concentration gradients, which are not observed here.

COS concentrations begin to rise at ~9:00, which marks the time when the boundary layer begins to rapidly grow and the 100 m inlet transitions from being above to within the boundary layer (Figure S10 in the supporting information). Surface measurements taken exclusively within the boundary layer (1–5 m), track the same general feature though appear to begin to rise slightly earlier than air samples from the upper inlet (Figure 7). Midday concentrations at 100 m reach values of up to 550 pmol mol^{-1} (Figure 8), exceeding ambient concentrations observed at the other sites. The rise in COS concentrations during the day toward the midday maxima occurs over a sustained period of many hours, which is in contrast to the rapid (1–2 h) transition observed at the other sites. The concentrations begin to steadily decrease at 16:00 and reach a nighttime minima near 3:00.

The COS and CO_2 concentrations at BAO fall along a single trajectory with an exponential shape (Figure 8). At this site, we assume the leaf flux is negligible—as there was insignificant green vegetation—and, as noted from the soil chamber experiments, the soil flux is generally driving the two gas species along a *positive* trajectory. It is therefore unlikely that soils alone could account for the covariation in these gases. While entrainment could drive the two gases along a negative trajectory as at the other sites (Figure 8), the impact of entrainment is a consequence of the recovery of COS and CO_2 concentrations following surface uptake, which cannot be called upon at a site without a surface sink. Based on this, we suggest that the statistically strong correlation between COS and CO_2 concentrations at this site are not causal, with CO_2 showing evidence of a similar, though more subdued, trend as the other sites, while COS is being controlled by another set of processes.

A number of lines of evidence suggest that there is a surface or regional source of COS influencing the concentrations at this site. Firstly, midday COS concentrations are generally higher than both GH and NWR (≥550 pmol mol^{-1}, Figure 8) and other sites in the Northern Hemisphere [*Montzka et al.*, 2007]. Secondly, measurements taken sequentially at 1, 3, and 5 m heights suggest there is a near-surface COS gradient, which would point toward a surface source (Figure 9). During the early morning (4–6:00 A.M.), there is very little COS gradient across the 10 m gradient, whereas CO_2 is elevated by about 10 μmol mol^{-1} at the surface. By midmorning (9–11:00 A.M.), the CO_2 gradient is no longer apparent, whereas COS at the surface is

now elevated by 30 pmol mol^{-1} relative to 10 m. Because the magnitude of the gradient is relaxed during the evening and grows during the early part of the day, it indicates the source of COS is likely dependent on temperature or radiation, as opposed to boundary layer dynamics. Measurements at the surface and 100 m were not made during the same days, so it is not feasible to calculate a surface to 100 m gradient, but there is some indication that the surface COS concentrations begin to rise earlier than at 100 m (Figure 7).

If we assume the observed positive slope between ambient COS concentrations and the COS flux from the soil is causal (Figure S9 in the supporting information), than, in theory, part of the observed diel cycle can be explained by fluxes from the soil [*Kesselmeier et al.*, 1999; *Kettle et al.*, 2002]. However, the sign of the soil flux across plots measured was heterogeneous and, on average, was close to zero, providing evidence that soil alone was not producing the flux that lead to the high ambient concentrations. Recent work by *Maseyk et al.* [2012] shows that senescent wheat stalks are a source of COS; it is thus plausible that the observed surface COS source is emission from inactive vegetation. We did not explicitly measure fluxes from the senescent grasses at BAO, though a cursory analysis of pine and aspen litter isolated from the soils at NWR did not reveal any COS emissions (Figure 4). Therefore, assuming all senescent vegetation emits COS is not warranted and additional efforts are needed to isolate the conditions and plant types that produce COS. It should also be noted that comprehensive chemical analyses on the air at the BAO by *Pétron et al.* [2012] reveal a number of sulfur species from various anthropogenic sources including gas/oil wells and landfills within the tower's large footprint [*LaFranchi et al.*, 2013]. However, both *Commane et al.* [2013] and *Belviso et al.* [2013] note that unlike CO_2 and CO, COS concentrations are not necessarily influenced by common industrial sources. Some evidence of this is shown in Figure 2 where transient rises in CO and CO_2 occasionally track one another, whereas COS is unresponsive to these short-lived phenomena.

4. Conclusions and Outlook

Carbonyl sulfide has been emerging recently as a possible tracer to constrain surface carbon exchange [*Blonquist et al.*, 2011] or other compounds such as biogenic VOCs. The results presented here combine a commercially available laser absorption spectrometer (LAS) with a branch bag gas exchange system and soil chamber, to rapidly characterize the COS flux across a wide range of species and soil conditions. The LAS approach has previously been validated [*Commane et al.*, 2013; *Asaf et al.*, 2013] and here a new instrument is tested and techniques are established to rapidly measure soil and leaf fluxes with simple gas exchange systems. A challenge in measuring COS fluxes and in inventorying natural sources and sinks is that its production from many common synthetic materials and industrial processes is unknown. This issue is mitigated here by using a completely stainless steel soil chamber and a branch bag whose surfaces are almost exclusively Teflon. However, COS emissions were detected both from the putty used to seal the branch bag and from the walls of the tanks used for storage of the references gases. These findings highlight that while COS has been measured for decades, critical inventorying of sources of COS remains vague and warrant careful decisions on materials used for field measurements. Furthermore, while the sensitivity of different LAS instruments to dynamic field conditions will vary, the temperature sensitivity of this instrument was significant and future studies would benefit from attempts to provide tighter controls of the instrument's operating environment.

The results across a variety of ecosystems agree with previous studies suggesting surface COS concentrations at photosynthetically active terrestrial sites are predominantly controlled by vegetation uptake [*Montzka et al.*, 2007; *Mihalopoulos et al.*, 1989] and that this process is stomatal controlled [*Sandoval-Soto et al.*, 2005; *Simmons et al.*, 1999; *Stimler et al.*, 2010a]. We are able to utilize this new field-based technology to significantly expand the existing database of discrete flask-GC-MS and laboratory experiments providing evidence that the normalized uptake ratio of COS to CO_2 (i.e., the LRU) is stable at 1.7 $\pm$ 0.3 across C3 genera [*Stimler et al.*, 2010a] (Table 1). This study provides strong evidence that the convergent LRU values observed in greenhouse and lab experiments holds across the diverse conditions tested in this study. As has been shown in some previous studies (e.g., *Protoschill-Krebs et al.* [1996]), we find there is significant nighttime uptake of COS from broad-leafed species (Figures 3 and 4). This arises because of incomplete stomatal closure (as well as *active* stomata opening during the night) coupled to the fact that the consumption of COS by carbonic anhydrase is not light dependent. The active opening of stomata prior to dawn is a known adaptation for plants to increase carbon fixation early in the day. While the use of COS as a proxy for GPP does not require tight constraints on nighttime COS uptake (i.e., GPP is zero), global model simulations of

COS that couple ecosystem and atmospheric transport models [e.g., *Berry et al.*, 2013] will be influenced by the representation of nocturnal COS cycling.

In agreement with some previous studies, we find that soils principally act as a COS sink [*Liu et al.*, 2010]. On the ecosystem scale, the magnitude of soil uptake in the forest and riparian sites studied here were significantly smaller than that from leaves. Although we are limited in our ability to quantitatively scale up the leaf measurements, our best estimates place this number between 2 and 6% of the leaf flux. If unaccounted for, soil fluxes would therefore generate only a small positive bias in GPP estimates derived from COS fluxes [*Asaf et al.*, 2013]. At night, soils generally play an important role in surface COS variability, though in regions dominated by broad-leafed species, the nighttime plant uptake could be comparable in magnitude to the soil flux. As with leaves, the relative uptake and emission of COS and CO_2 by soils can be normalized to background concentrations and modeled as a function of temperature, denoted as SRU here (Figure 6). Evidence of a fairly simple uptake ratio of COS to CO_2 in soils emerges despite the fact that the response of both COS and CO_2 fluxes to temperature, moisture, and background ambient concentrations interact in nonlinear ways. For example, during the highest temperatures, we observed both instances of the highest uptake and emission fluxes of COS. We acknowledge that some of the complexity of the response of COS to temperatures observed here may be a product of the fact that temperatures were measured in the air space above the soil, while carbonic anhydrase activity may be maximized at depth [*Wingate et al.*, 2009]. The results from the soil fluxes at BAO, a senescent grassland site, challenge the notion that a simple empirical relationship between COS and CO_2 fluxes (i.e., SRU) could be adopted in models. The fluxes from these soils were small and not well constrained by any obvious empirical relationships and may reflect emissions from senescent plant stalks that are incorporated into the soil.

Understanding the diel evolution of the covariation between COS and CO_2 in the ambient surface air (Figure 8) could be used to partition the relative importance that soil, leaf, and atmospheric dynamics have on surface carbon exchange. An example of the utility of synchronous ambient COS and CO_2 measurements is observed during the early morning at the NWR and GH sites when CO_2 concentrations experience a rapid decline, which we identify using COS measurements to be almost exclusively the result of plant uptake. The significant carbon uptake by plants early in the morning is common in many plant species (particularly when stressed by high midday vapor pressure deficits) and is poorly constrained by eddy covariance as turbulence is weak during this period of the day. The slope between COS and CO_2 is soon reversed, during the midday growth of the boundary layer, at which point entrainment of COS-rich and CO_2-depleted air occurs. Partitioning the role of surface processes on the COS budget is not trivial in instances where changes in the geometry of the footprint delivers air of variable COS concentrations. However, changes in air mass origin likely played only a minimal role on the diel cycles in the sites studied here and unlike CO_2, which was influenced by emissions from cars (Figure 2), COS seemed largely immune to common anthropogenic activity [*Commane et al.*, 2013; *Belviso et al.*, 2013].

The data from a senescent grassland (BAO) provide an important contrast to the results obtained from the active forest and riparian settings (NWR and GH, respectively). COS concentrations at BAO are inherently distinct from the other sites and confirm that the absence of active vegetation and soils significantly alter the surface COS budget. The results from BAO strongly suggest the presence of a terrestrial COS source (Figure 9), though its origin remains unknown. While additional measurements of COS using field-based laser absorption techniques will likely shed light on these sources, their presence does not negate the potential power continuous COS measurements provide in understanding first-order properties of surface carbon exchange in active ecosystems [*Asaf et al.*, 2013] and in constraining new efforts to model this gas on the global scale [*Berry et al.*, 2013].

References

Asaf, D., E. Rotenberg, F. Tatarinov, U. Dicken, S. A. Montzka, and D. Yakir (2013), Ecosystem photosynthesis inferred from measurements of carbonyl sulphide flux, *Nat. Geosci.*, 6(3), 186–190.

Aubinet, M., C. Feigenwinter, B. Heinesch, C. Bernhofer, E. Canepa, A. Lindroth, L. Montagnani, C. Rebmann, P. Sedlak, and E. Van Gorsel (2010), Direct advection measurements do not help to solve the night-time CO_2 closure problem: Evidence from three different forests, *Agric. For. Meteorol.*, 150(5), 655–664.

Baldocchi, D. (1997), Flux footprints within and over forest canopies, *Boundary Layer Meteorol.*, 85(2), 273–292.

Baldocchi, D., et al. (2001), Fluxnet: A new tool to study the temporal and spatial variability of ecosystem-scale carbon dioxide, water vapor, and energy flux densities, *Bull. Am. Meteorol. Soc.*, 82(11), 2415–2434.

Ballantyne, A., C. Alden, J. Miller, P. Tans, and J. White (2012), Increase in observed net carbon dioxide uptake by land and oceans during the past 50 years, *Nature*, 488(7409), 70–72.

Barford, C., S. Wofsy, M. Goulden, J. Munger, E. Pyle, S. Urbanski, L. Hutyra, S. Saleska, D. Fitzjarrald, and K. Moore (2001), Factors controlling long- and short-term sequestration of atmospheric CO_2 in a mid-latitude forest, *Science*, *294*(5547), 1688–1691.

Beer, C., et al. (2010), Terrestrial gross carbon dioxide uptake: Global distribution and covariation with climate, *Science*, *329*(5993), 834–838.

Belviso, S., M. Schmidt, C. Yver, M. Ramonet, V. Gros, and T. Launois (2013), Strong similarities between night-time deposition velocities of carbonyl sulphide and molecular hydrogen inferred from semi-continuous atmospheric observations in Gif-sur-Yvette, Paris region, *Tellus B*, *65*, 20,719.

Berkelhammer, M., J. Hu, A. Bailey, D. Noone, B. Still, H. Barnard, D. Gochis, G. Hsiao, and A. Turnipseed (2013), Nocturnal water cycling in an open-canopy forest, *J. Geophys. Res. Atmos.*, *118*, 10,225–10,242, doi:10.1002/jgrd.50701.

Berry, J., et al. (2013), A coupled model of the global cycles of carbonyl sulfide and CO_2: A possible new window on the carbon cycle, *J. Geophys. Res. Biogeosci.*, *118*, 842–852, doi:10.1002/jgrg.20068.

Blonquist, J., Jr., S. Montzka, J. Munger, D. Yakir, A. Desai, D. Dragoni, T. Griffis, R. Monson, R. Scott, and D. Bowling (2011), The potential of carbonyl sulfide as a proxy for gross primary production at flux tower sites, *J. Geophys. Res.*, *116*, G04019, doi:10.1029/2011JG001723.

Caird, M., J. Richards, and L. Donovan (2007), Nighttime stomatal conductance and transpiration in C3 and C4 plants, *Plant Physiol.*, *143*(1), 4–10.

Campbell, J., et al. (2008), Photosynthetic control of atmospheric carbonyl sulfide during the growing season, *Science*, *322*(5904), 1085–1088.

Commane, R., S. Herndon, M. Zahniser, B. Lerner, J. McManus, J. Munger, D. Nelson, and S. Wofsy (2013), Carbonyl sulfide in the planetary boundary layer: Coastal and continental influences, *J. Geophys. Res. Atmos.*, *118*(14), 8001–8009, doi:10.1002/jgrd.50581.

Fisher, J., D. Baldocchi, L. Misson, T. Dawson, and A. Goldstein (2007), What the towers don't see at night: Nocturnal sap flow in trees and shrubs at two AmeriFlux sites in California, *Tree Physiol.*, *27*(4), 597–610.

Friedlingstein, P., et al. (2006), Climate-carbon cycle feedback analysis: Results from the C4MIP model intercomparison, *J. Clim.*, *19*(14), 3337–3353.

Gu, L., et al. (2005), Objective threshold determination for nighttime eddy flux filtering, *Agric. For. Meteorol.*, *128*(3), 179–197.

Harley, P., L. Otter, A. Guenther, and J. Greenberg (2003), Micrometeorological and leaf-level measurements of isoprene emissions from a Southern African savanna, *J. Geophys. Res.*, *108*(D13), 8468, doi:10.1029/2002JD002592.

Heath, O. (1984), Stomatal opening in darkness in the leaves of Commelina communis, attributed to an endogenous circadian rhythm: Control of phase, *Proc. R. Soc. London, Ser. B*, *220*(1221), 399–414.

Kesselmeier, J., N. Teusch, and U. Kuhn (1999), Controlling variables for the uptake of atmospheric carbonyl sulfide by soil, *J. Geophys. Res.*, *104*(D9), 11,577–11,584.

Kettle, A., U. Kuhn, M. Von Hobe, J. Kesselmeier, and M. Andreae (2002), Global budget of atmospheric carbonyl sulfide: Temporal and spatial variations of the dominant sources and sinks, *J. Geophys. Res.*, *107*(D22), 4658, doi:10.1029/2002JD002187.

Kuhn, U., C. Ammann, A. Wolf, F. Meixner, M. Andreae, and J. Kesselmeier (1999), Carbonyl sulfide exchange on an ecosystem scale: Soil represents a dominant sink for atmospheric COS, *Atmos. Environ.*, *33*(6), 95–1008.

LaFranchi, B., et al. (2013), Constraints on emissions of carbon monoxide, methane, and a suite of hydrocarbons in the Colorado Front Range using observations of $^{14}CO_2$, *Atmos. Chem. Phys. Discuss.*, *13*(1), 1609–1672.

Lasslop, G., M. Reichstein, D. Papale, A. Richardson, A. Arneth, A. Barr, P. Stoy, and G. Wohlfahrt (2009), Separation of net ecosystem exchange into assimilation and respiration using a light response curve approach: Critical issues and global evaluation, *Global Change Biol.*, *16*(1), 187–208.

Lavigne, M., et al. (1997), Comparing nocturnal eddy covariance measurements to estimates of ecosystem respiration made by scaling chamber measurements at six coniferous boreal sites, *J. Geophys. Res.*, *103*, 28–28.

Liu, J., C. Geng, Y. Mu, Y. Zhang, Z. Xu, and H. Wu (2010), Exchange of carbonyl sulfide (COS) between the atmosphere and various soils in China, *Biogeosciences*, *7*, 753–726.

Loescher, H., B. Law, L. Mahrt, D. Hollinger, J. Campbell, and S. Wofsy (2006), Uncertainties in, and interpretation of, carbon flux estimates using the eddy covariance technique, *J. Geophys. Res.*, *111*(D10), D21S90, doi:10.1029/2005JD006932.

Maseyk, K., U. Seibt, J. Berry, D. Billesbach, E. Campbell, and M. Torn (2012), Strong soil source of carbonyl sulfide in an agricultural field, Abstract B44A-04 presented at 2012 Fall Meeting, AGU, San Francisco, Calif., 3–7 Dec.

Mihalopoulos, N., B. Bonsang, B. Nguyen, M. Kanakidou, and S. Belviso (1989), Field observations of carbonyl sulfide deficit near the ground: Possible implication of vegetation, *Atmos. Environ.*, *23*(10), 2159–2166.

Miller, J. B., D. Yakir, J. W. White, and P. P. Tans (1999), Measurement of $^{18}O/^{16}O$ in the soil-atmosphere CO_2 flux, *Global Biogeochem. Cycles*, *13*(3), 761–774.

Monson, R., A. Turnipseed, J. Sparks, P. Harley, L. Scott-Denton, K. Sparks, and T. Huxman (2002), Carbon sequestration in a high-elevation, subalpine forest, *Global Change Biol.*, *8*(5), 459–478.

Montzka, S., P. Calvert, B. Hall, J. Elkins, T. Conway, P. Tans, and C. Sweeney (2007), On the global distribution, seasonality, and budget of atmospheric carbonyl sulfide (COS) and some similarities to CO_2, *J. Geophys. Res.*, *112*, D09302, doi:10.1029/2006JD007665.

Nagler, P. L., E. P. Glenn, T. Lewis Thompson, and A. Huete (2004), Leaf area index and normalized difference vegetation index as predictors of canopy characteristics and light interception by riparian species on the Lower Colorado River, *Agric. For. Meteorol.*, *125*(1), 1–17.

Pétron, G., et al. (2012), Hydrocarbon emissions characterization in the Colorado Front Range: A pilot study, *J. Geophys. Res.*, *117*(D4), D04304, doi:10.1029/2011JD016360.

Protoschill-Krebs, G., C. Wilhelm, and J. Kesselmeier (1996), Consumption of carbonyl sulphide (COS) by higher plant carbonic anhydrase (CA), *Atmos. Environ.*, *30*(18), 3151–3156.

Provencal, R., G. Gupta, D. Baer, and B. Genty (2012), Ultrasensitive analyzer for realtime, in-situ airborne and terrestrial measurements of OCS, CO_2, CO, and H_2O, Abstract B51B-0529 presented at 2012 Fall Meeting, AGU, San Francisco, Calif., 13–17 Dec.

Qi, Y., M. Xu, and J. Wu (2002), Temperature sensitivity of soil respiration and its effects on ecosystem carbon budget: Nonlinearity begets surprises, *Ecol. Modell.*, *153*(1), 131–142.

Sandoval-Soto, L., M. Stanimirov, M. Von Hobe, V. Schmitt, J. Valdes, A. Wild, and J. Kesselmeier (2005), Global uptake of carbonyl sulfide (COS) by terrestrial vegetation: Estimates corrected by deposition velocities normalized to the uptake of carbon dioxide (CO_2), *Biogeosciences*, *2*(2), 125–132.

Scanlon, T., and W. Kustas (2010), Partitioning carbon dioxide and water vapor fluxes using correlation analysis, *Agric. For. Meteorol.*, *150*(1), 89–99.

Schimel, D., et al. (2001), Recent patterns and mechanisms of carbon exchange by terrestrial ecosystems, *Nature*, *414*, 169–172.

Seibt, U., J. Kesselmeier, L. Sandoval-Soto, U. Kuhn, and J. Berry (2010), A kinetic analysis of leaf uptake of COS and its relation to transpiration, photosynthesis and carbon isotope fractionation, *Biogeosciences*, *7*, 333–341.

Simmons, J., L. Klemedtsson, H. Hultberg, and M. Hines (1999), Consumption of atmospheric carbonyl sulfide by coniferous boreal forest soils, *J. Geophys. Res.*, *104*(D9), 11,569–11,576.

Stimler, K., S. Montzka, J. Berry, Y. Rudich, and D. Yakir (2010a), Relationships between carbonyl sulfide (COS) and CO_2 during leaf gas exchange, *New Phytol.*, *186*(4), 869–878.

Stimler, K., D. Nelson, and D. Yakir (2010b), High precision measurements of atmospheric concentrations and plant exchange rates of carbonyl sulfide using mid-IR quantum cascade laser, *Global Change Biol.*, *16*(9), 2496–2503.

Urbanski, S., C. Barford, S. Wofsy, C. Kucharik, E. Pyle, J. Budney, K. McKain, D. Fitzjarrald, M. Czikowsky, and J. Munger (2007), Factors controlling CO_2 exchange on timescales from hourly to decadal at Harvard Forest, *J. Geophys. Res.*, *112*(G2), G02020, doi:10.1029/2006JG000293.

Van Diest, H., and J. Kesselmeier (2008), Soil atmosphere exchange of carbonyl sulfide (COS) regulated by diffusivity depending on water-filled pore space, *Biogeosciences*, *5*(2), 475–483.

Wilson, K., et al. (2002), Energy balance closure at FLUXNET sites, *Agric. For. Meteorol.*, *113*(1), 223–243.

Wingate, L., et al. (2009), The impact of soil microorganisms on the global budget of $\delta^{18}O$ in atmospheric CO_2, *PNAS*, *106*(52), 22,411–22,415.

Wohlfahrt, G., F. Brilli, L. Hörtnagl, X. Xu, H. Bingemer, A. Hansel, and F. Loreto (2012), Carbonyl sulfide (COS) as a tracer for canopy photosynthesis, transpiration and stomatal conductance: Potential and limitations, *Plant Cell Environ.*, *35*(4), 657–67.

Xu, L., M. D. Furtaw, R. A. Madsen, R. L. Garcia, D. J. Anderson, and D. K. McDermitt (2006), On maintaining pressure equilibrium between a soil CO_2 flux chamber and the ambient air, *J. Geophys. Res.*, *111*(D8), D08S10, doi:10.1029/2005JD006435.

Yakir, D., and X. Wang (1996), Fluxes of CO_2 and water between terrestrial vegetation and the atmosphere estimated from isotope measurements, *Nature*, *380*(6574), 515–517.